FEASIBILITY STUDY OF MICROPHONE PHASED ARRAY BASED MACHINERY HEALTH MONITORING

Patricio Ravetta [a], Jorge Muract [a], and Ricardo Burdisso[b]

[a]*AVEC, Inc., 2000 Kraft Drive, Suite 1109, Virginia Tech Corporate Research Center, Blacksburg, VA, 24060, USA, pravetta@avec-engineering.com, www.avec-engineering.com*
[b]*Professor, Vibration and Acoustics Lab, Virginia Tech, 153 Durham Hall, Blacksburg, VA, 24060, USA, rburdiss@vt.edu*

Keywords: Microphone Phased Arrays, Machine Health Monitoring, Modeling.

Abstract. To increase reliability and safety, industrial plant equipment such as compressors, electric motors, gear trains, and so forth are regularly monitored for damage. A traditional approach for monitoring is for a trained technician to make vibration measurements of the equipment. Inspection of the vibration measurements and their comparison to known healthy/damaged data sets allow for assessing the health status of the machines. This process is repeated at regular intervals. However, it is time-consuming and labor-intensive. It would be greatly convenient both in terms of time and cost to develop a remote acoustic based system to detect the health status of industrial equipment. A microphone phased array machine health monitoring system is proposed to remotely identify and classify machine faults. Acoustic spectral signature analysis has existed for many years, and it is similar to vibration analysis using accelerometers with the advantage that nothing must be mounted on the machine. In addition, acoustic imaging systems using microphone phased arrays have also been in existence for many years. The current state-of-the-art, however, requires an expert human operator to interpret the data from these devices, and therefore it is not suitable for automated, online monitoring. The implementation of a microphone phased array approach to monitor equipment faults in a typical industrial environment presents some unique challenges. A typical industrial plant is a highly acoustic reverberant environment that will result in significant reflections and background noise levels. To be effective, the array will need to be able to monitor multiple machines through the plant, simultaneously. To investigate the potential of the proposed approach, a numerical model of the microphone phased array in a large highly reverberant room was developed. The model was then used to investigate several array designs, study the effect of reflections and reverberation, determine the capability of the system to monitor multiple machines and so forth. These numerical studies revealed that the critical concern is that the array signal to noise ratio must be larger than the noise difference between the loudest and quietest machines being monitored. It was also found that the reverberation of typical industrial plants is not important if a sufficient number of microphones is used in the array, e.g. for a plant with an average absorption coefficient of 10% a minimum of 100 microphones is required in the array.

1 INTRODUCTION

Industrial plant equipment such as compressors, electric motors, gears, and so forth are regularly monitored for the detection of faults. The classic approach for monitoring is for a trained technician to make vibration measurements of the equipment in the plant. Inspection of the vibration measurements and comparison to known healthy/damaged data allow assessing the health status of the machines. It would be greatly convenient both in terms of time and cost to develop a remote acoustic based system to detect rotating equipment health status. Acoustic spectral signature analysis has existed for many years, and is similar to vibration analysis using accelerometers with the advantage that the sensors do not need to be mounted on the machine. Acoustic imaging systems using microphone phased arrays have also been in existence for some time (Brooks et.al., 1987; Grosche, et.al., 1997; Herkes and Stoker, 1998; Sijtsma Holthusen, 1999). The health monitoring of machinery using acoustic imaging technique is the subject of this work.

The implementation of a microphone phased array approach to monitor equipment faults in a typical industrial environment presents some unique challenges. A typical industrial plant is a highly acoustically reverberant environment that will result in significant reflections and background noise levels. In addition, the feasible system will need to be able to monitor multiple machines. Finally, the monitoring should not interfere with the normal operation of the machines as well as its maintenance.

This work investigates the feasibility study of using microphone phased array technology for health monitoring of industrial equipment as illustrated in Figure 1. The microphone phased array is positioned at a location that gives a direct line of sight to the equipment to be monitored, i.e. hanging from the ceiling of the high-bay room as a permanent eye-in-the-sky position. The microphone phased array will have a large number of microphones depending on the array signal-to-noise-ratio (SNR) required. The signals from the microphones are then used to generate an acoustic image of the source known as "beamforming" (Johnson and Dudgeon, 1993). The main goal of beamforming over the volume enclosing the piece of equipment is to "capture" all the noise sources from the unit being monitored. This beamforming process produces acoustic images (as a function of frequency) which are conventionally used to identify individual noise sources by an expert human operator (Ravetta, et.al., 2004). To aid in the interpretation of the results and automate the damage identification process, the acoustic images are integrated to produce a representative spectrum of the noise signature of the piece of equipment as observed by the array (Mueller, 2002). The "measured integrated" equipment spectrum will be used to identify damage. To this end, the "integrated" spectrum should be compared to the spectrum of the healthy system or the spectrum of known faults.

Though a first impression of the proposed technology seems straight forward, a closer look reveals a number of technical challenges that need to be considered and investigated. Examples of these issues are contamination of the "integrated" spectrum due to other machines, uncorrelated noise due to reverberation in typical of industrial facilities, and so forth.

The main goal of this work is to investigate the feasibility of the microphone phased array system to monitor the health of plant equipment in a realistic environment. To this end, a numerical model was developed and used to investigate the effect of key variables

of the system, e.g. reflections, room absorption, number of microphones and size of the array, and so forth.
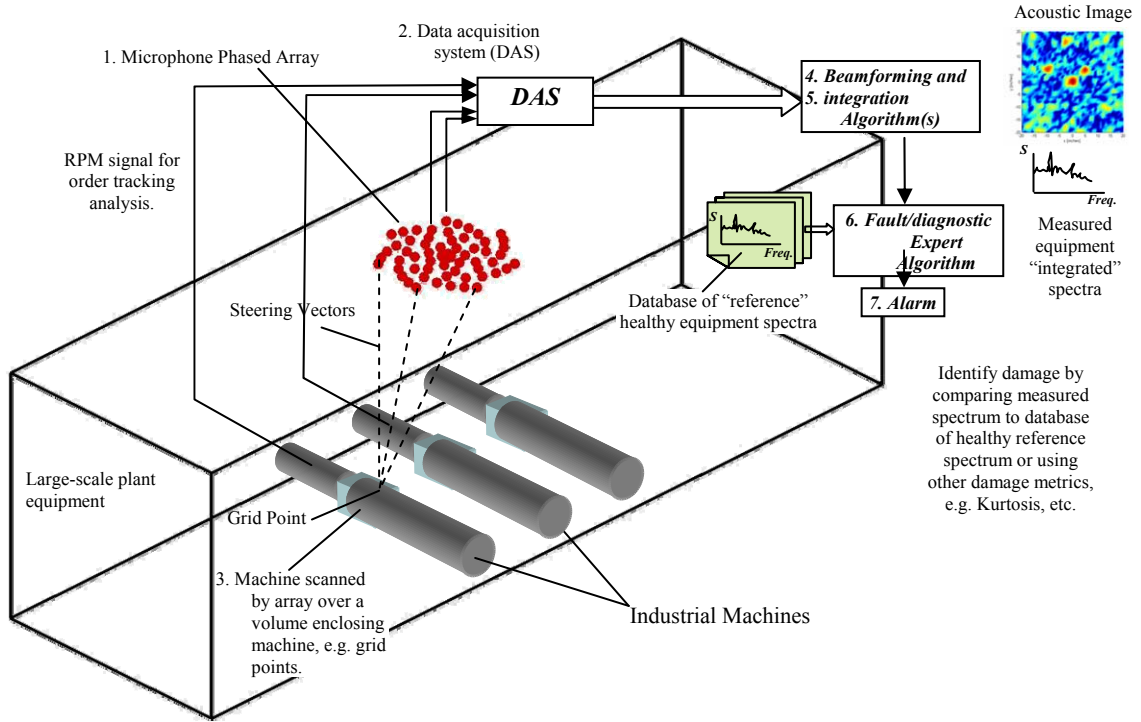
Figure 1: Illustration of 2D microphone phased array health monitoring system for plant equipment.

2 MODELING OF PHASED ARRAY HEALTH MONITORING SYSTEM

In this section, the numerical model developed to simulate the proposed fault diagnostic system is presented. The model can simulate the plant environment including reverberation and reflections, multiple machines, any array design, and simple machine damage scenarios. To develop the model, it is necessary to understand and capture the characteristic of the sound field in a highly reverberant room of typical industrial plants. In a room with reflective surfaces multiple reflections occur and a uniform reverberant field is established in addition to the direct radiation. The level of the reverberant field depends on the room sound absorption, i.e. low sound absorption typical of industrial plants leads to higher reverberation levels.

For simplicity, the numerical model is developed in the frequency domain. The industrial plant was modeled as a rectangular room with dimensions L_x, L_y, and L_z as shown in Figure 2. It is assumed that inside this industrial plant there is an array of machines simulating equipment being monitored, e.g. electric motor, gearbox, and compressor. The main goal is to monitor the health of these machines using a microphone phased array installed on the ceiling such as to have an unobstructed direct line of sight to the machines to be monitored, i.e. eye-in-the-sky configuration.
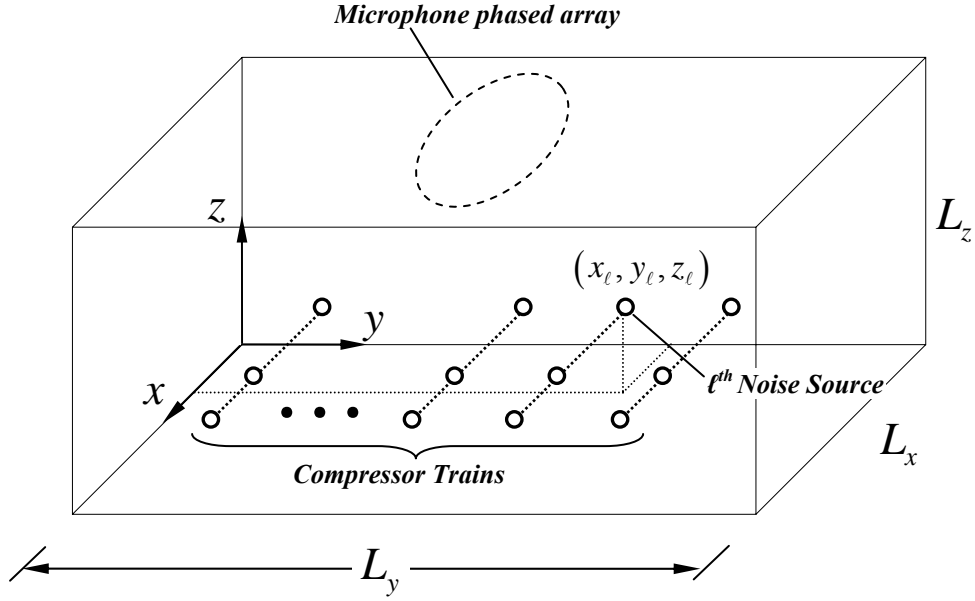
Figure 2: High-bay industrial plant modeled as a rectangular room. Noise from array of machines (e.g. motor/gear/compressor) modeled as monopole noise sources.

The model needs to predict the sound field measured by the microphones in the array due to the noise sources present in the room. To this end, there are several approaches that could have been taken such as Green's functions, image method, finite and boundary element methods, and so forth. Due to the large size of the room, Green's functions and numerical methods are computationally intensive and thus impractical. The image method can also be unworkable if all possible reflections are modeled, i.e. it will require an excessive number of "image" sources. The modeling approach used here was based on the statistical energy analysis used in room acoustics which is valid at frequencies above the cross-over frequency (Bies and Hansen, 1986). The cross-over frequency for a typical industrial plant is normally very low (<100 Hz).

The modeling approach used here is to predict direct and reverberant sound fields independently. The direct field is the sound from a source propagating until the first reflection occurs. The reflected sound is then considered part of the reverberant field. Thus, the direct field can be easily computed assuming the source is in free field, i.e. no boundaries. The direct sound field contains information in terms of both magnitude and phase. On the other hand, the reverberant field is assumed to be uncorrelated from the direct field due to the reflections/scattering effects. The reverberant field is also assumed not to have a spatial correlation and it is basically uniform. Thus, the reverberant sound field behaves as background noise contaminating the direct field and providing no relevant information to the microphone phased array. In addition, the following modeling assumptions are made: (i) the reflection and diffraction effects of the machinery will be ignored and (ii) the noise sources in the room will be modeled as monopoles, i.e. omni-directional radiation.

Thus, the sound field at a point $\vec{r}_o = (x_o, y_o, z_o)$ in the room due to a single monopole source located at $\vec{r}_\ell = (x_\ell, y_\ell, z_\ell)$ becomes

$$p(\vec{r}_o | \vec{r}_\ell, f) = p_D(\vec{r}_o | \vec{r}_s, f) + p_R(\vec{r}_o, f) = \left| p_D(\vec{r}_o | \vec{r}_\ell, f) \right| e^{i\phi_D(f)} e^{i2\pi f t} + \left| p_R(\vec{r}_o, f) \right| e^{i\phi_R(f)} e^{i2\pi f t} \quad (1)$$

where $p_D(\vec{r}_o | \vec{r}_s, f)$ is the complex pressure due to direct field; $p_R(\vec{r}_o, f)$ is the complex pressure due to reverberant field; $\phi_D(f)$ and $\phi_R(\vec{r}_o, f)$ are the phase angles of the direct and reverberant fields; and f is the frequency. Note that the phase of the reverberant pressure $\phi_R(\vec{r}_o, f)$ is assumed to vary randomly from point to point in the room, i.e. spatially uncorrelated. The time dependant term $e^{i2\pi f t}$ is omitted in the rest of the formulation.

The direct sound field at $\vec{r}_o$ due to the monopole source located at $\vec{r}_\ell$ is easily computed as

$$p_D(\vec{r}_o | \vec{r}_\ell, f) = \frac{A_\ell(f)}{|\vec{r}_o - \vec{r}_\ell|} e^{-ik|\vec{r}_o - \vec{r}_\ell|} \quad (2)$$

where $k = \dfrac{2\pi f}{c}$ is the acoustic wavenumber, c is the speed of sound, and $A_\ell(f)$ is the complex amplitude of the monopole source. The magnitude of the source amplitude can be computed knowing the source sound power $W_\ell(f)$ as follows (Ravetta, et.al. 2006).

$$\left| A_\ell(f) \right| = \sqrt{\frac{W_\ell(f)\rho c}{2\pi}} \quad (3)$$

where ρc is the acoustic impedance of air. The phase of the complex amplitude $\varphi_\ell(f)$ will be assumed known.

The reverberant component can be computed from the acoustic power in the room and the room acoustic properties as

$$\left(p_{rms}^2(f) \right)_R = \frac{1 - \overline{\alpha}_{plant}(f)}{S \overline{\alpha}_{plant}(f)} = \frac{W_\ell(f) 4\rho c}{R(f)} \quad (4)$$

where S is the room's internal surface and $\overline{\alpha}_{plant}(f)$ is the plant average absorption coefficient. In practice, the absorption coefficient is experimentally determined from the room reverberation time, $T_{60}(f)$. The typical absorption of a large industrial plant without noise treatment is most likely below 0.2.

Note that equation (4) allows only to compute the magnitude, $\left| p_R(f) \right|$, of the reverberant component . The phase angle $\phi_R(\vec{r}_o, f)$ is assumed to be a random variable. Note that to model background noise that is spatially uncorrelated, the seed for the generation of the random phase is different at each location.

To model the array and beamforming process, the cross spectral matrix (CSM) is required and it is given as (Mosher, 1996)

$$[A] = \left\{ p_{MPA}(\vec{r}_\ell) \right\} \left\{ p_{MPA}(\vec{r}_\ell) \right\}^H \quad (6)$$

where $\left\{ p_{MPA}(\vec{r}_\ell) \right\}$ is a vector whose components represent the acoustic pressure produced

by the monopole source at each microphone in the array. Therefore, the components of the vector $\{p_{MPA}(\vec{r}_\ell)\}$ are given by eq. (1) evaluated at the positions of the microphones in the array. The superscript H applied to a vector or matrix indicate the Hermitian, i.e. transposed and complex conjugate.

The vector $\{p_{MPA}(\vec{r}_\ell)\}$ can be written as

$$\{p_{MPA}(\vec{r}_\ell)\} = \{p_{MPA}(\vec{r}_\ell)\}_D + \{p_{MPA}(\vec{r}_\ell)\}_R \tag{7}$$

where

$$\{p_{MPA}(\vec{r}_\ell)\}_D = A_\ell(f) \left\{ \frac{e^{-ik|\vec{r}_1-\vec{r}_\ell|}}{|\vec{r}_1-\vec{r}_\ell|}, \cdots, \frac{e^{-ik|\vec{r}_m-\vec{r}_\ell|}}{|\vec{r}_m-\vec{r}_\ell|}, \cdots, \frac{e^{-ik|\vec{r}_M-\vec{r}_\ell|}}{|\vec{r}_M-\vec{r}_\ell|} \right\}^T \tag{8}$$

and

$$\{p_{MPA}(\vec{r}_\ell)\}_R = \sqrt{\frac{2W_\ell(f)4\rho c}{R(f)}} \left\{ e^{i\phi_R(\vec{r}_1)}, \cdots, e^{i\phi_R(\vec{r}_m)}, \cdots, e^{i\phi_R(\vec{r}_M)} \right\}^T \tag{9}$$

are the vectors of complex pressures at each microphone due to the direct and reverberant components, respectively. The number of microphones in the array is M.

Replacing (7) into (6) yields a cross spectral matrix that is the linear contribution of four components as

$$[A] = [A_{DD}] + [A_{RR}] + [A_{DR}] + [A_{RD}]$$

$$[A] = \{p_{MPA}(\vec{r}_\ell)\}_D \{p_{MPA}(\vec{r}_\ell)\}_D^H + \{p_{MPA}(\vec{r}_\ell)\}_R \{p_{MPA}(\vec{r}_\ell)\}_R^H \tag{10}$$

$$+ \{p_{MPA}(\vec{r}_\ell)\}_D \{p_{MPA}(\vec{r}_\ell)\}_R^H + \{p_{MPA}(\vec{r}_\ell)\}_R \{p_{MPA}(\vec{r}_\ell)\}_D^H$$

Based on the assumption that the direct and reverberant fields are uncorrelated, the last two matrices in (10) would vanish. Moreover, from the assumption that the reverberant field is spatially uncorrelated, the 2nd matrix would then be diagonal. However, these assumptions are not realistic and likely there is some degree of correlation (both between direct and reverberant fields as well as spatially for the reverberant component). To account for this partial correlation, it is assumed that the cross spectral matrix is computed as the average of N_a computations of equation (10) with the phase of the reverberant field at each microphone location varying randomly. That is, the phases $\phi_R(\vec{r}_n) \quad n = 1, 2, \ldots, M$ are random variables. Thus, the (n,m) term of each of the matrices defining the cross spectral matrix are given as

$$A_{DD}(n,m) = |A_\ell(f)|^2 \frac{e^{-ik|\vec{r}_n-\vec{r}_\ell|}}{|\vec{r}_n-\vec{r}_\ell|} \frac{e^{ik|\vec{r}_m-\vec{r}_\ell|}}{|\vec{r}_m-\vec{r}_\ell|} = \frac{W_\ell \rho c}{2\pi} \frac{e^{-ik|\vec{r}_n-\vec{r}_\ell|}}{|\vec{r}_n-\vec{r}_\ell|} \frac{e^{ik|\vec{r}_m-\vec{r}_\ell|}}{|\vec{r}_m-\vec{r}_\ell|} \tag{11}$$

$$A_{RR}(n,m) = \frac{W_\ell 16\pi}{R(f)} \frac{1}{N_a} \sum_{na=1}^{N_a} e^{i\left[\phi_R^{na}(\vec{r}_n^s) - \phi_R^{na}(\vec{r}_m^s)\right]} \tag{12}$$

$$A_{DR}(n,m) = A_{RD}^*(n,m) = \frac{1}{N_a} \sum_{na=1}^{N_a} \frac{A_\ell e^{-ik|\vec{r}_n-\vec{r}_\ell|}}{|\vec{r}_n-\vec{r}_\ell|} \sqrt{\frac{2W_\ell(f)4\rho c}{R(f)}} e^{i\phi_R^{na}(\vec{r}_m)} \tag{13}$$

or using (3) gives

$$A_{DR}(n,m) = A_{RD}^*(n,m) = W_\ell(f)\sqrt{\frac{4}{\pi R(f)}} \frac{\rho c}{|\vec{r}_n - \vec{r}_\ell|} \frac{1}{N_a} \sum_{na=1}^{N_a} e^{-i\left(k|\vec{r}_n - \vec{r}_\ell| + \phi_R^{na}(\vec{r}_m)\right)} \quad (14)$$

where $\phi_R^{na}(\vec{r}_n)$ is the na^{th} sample of the random sequence ($na = 1, 2, \ldots, N_a$) of the phase of the reverberant field at the nth microphone of the array.

It is interesting to note that the summations in (12) and (14) are the complex addition of unit vectors of random phase. As the number of averages increases the summations are given by

$$N_a \rightarrow \infty \quad \therefore \begin{cases} \dfrac{1}{N_a} \displaystyle\sum_{na=1}^{N_a} e^{i\left[\phi_R^{na}(\vec{r}_n^s) - \phi_R^{na}(\vec{r}_m^s)\right]} \rightarrow \begin{cases} 1 & n = m \\ 0 & n \neq m \end{cases} \\[4mm] \dfrac{1}{N_a} \displaystyle\sum_{na=1}^{N_a} e^{-i\left(k|\vec{r}_n - \vec{r}_\ell| + \phi_R^{na}(\vec{r}_m)\right)} \rightarrow 0 \end{cases} \quad (15)$$

which corresponds to the perfectly correlated or uncorrelated cases.

The sound field produced by multiple noise sources inside the plant can be easily extended from the previous derivation. The derivation details can be found in the work of Ravetta, et.al. (2006).

It is important to note that the model presented here can also be used to determine the requirements for the data acquisition system to be used in this application, e.g. dynamic range, resolution, maximum levels to be recorded. For example, the term $10Log_{10}(A_{DD}/A_{RR})$ is the microphone signal to noise ratio while the diagonal of matrix [A] can be used to compute the maximum noise levels to be recorded by the microphones.

It is important to incorporate into the model reflection effects from the room's boundary. The image method approach is used to model the first reflection as shown in Figure 3. In this example, the sound from the ℓth source gets reflected on the plane defined by $z=0$. This reflection is accounted for using an image source positioned on the other side of this plane. The same source will also produce a first reflection on the other four planes, i.e. planes defined by $x = 0, L_x$, and $y = 0, L_y$ (not shown in the figure). The direct and reflected acoustic pressures at the nth microphone position on the ceiling are also indicated in the figure and can be easily computed considering the ℓth source and its image as perfectly correlated.

If the first reflections are accounted for as explained, the contribution of the first reflections should be removed from the reverberant field. Since the amount of sound absorption is assumed small (i.e. there is no acoustic treatment), the reduction in the reverberant field is likely not significant. Thus, in this model the reverberant field is not corrected by accounting for the first reflections. Note that this assumption is conservative since the reverberant field is being overestimated.
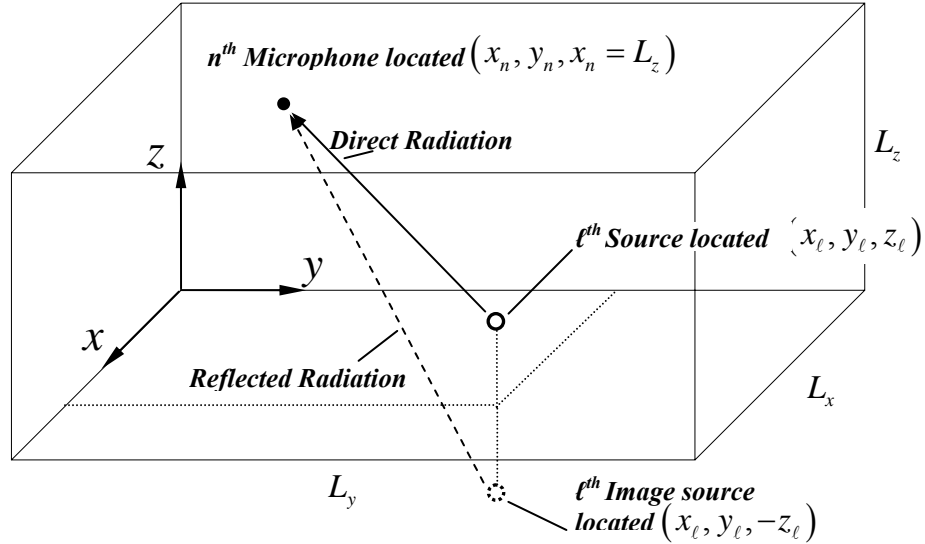
Figure 3: Illustration of the image method approach used to account for reflection effects. Figure only shows the reflection from the plane defined by $z = 0$.

3 NUMERICAL SIMULATIONS

The model was implemented and used to investigate the effect of critical system parameters. The industrial plan was assumed to have room dimensions of 30x30x100 meters. In all cases, the array was positioned at the center of the ceiling as shown in Figure 4. Using this model of a room, the performance of several array designs was investigated. To this end, 12 different microphone phased arrays were designed and investigated. It was decided to fix the outside diameter of the array to 20 meters so that it would easily fit on the ceiling of the room modeled. A large diameter array will also allow a good resolution at low frequencies. Because it is known to be a robust design, it was also decided to use a 7-arm equal-aperture spiral pattern for all array designs.
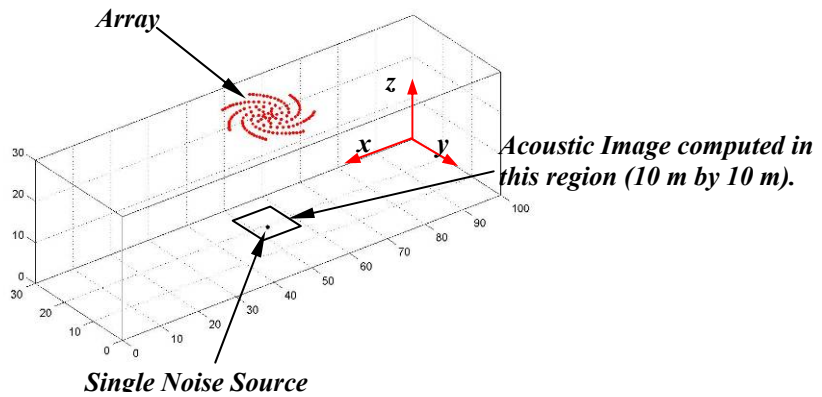
Figure 4: Schematic of room indicating grid where acoustic image was computed.

3.1 Phased Array Performance

The performance of the array designs is determined by investigating the array signal-to-noise ratio (SNR) and the beamwidth (BW). To this end, acoustic images for a single

source positioned at the location shown in Figure 4 (x=50,y=15,z=3) were computed over a 10 m by 10 m grid. The acoustic images were computed for a frequency range from 100 to 6000 Hz. The room sound absorption coefficient was assumed to be $\bar{\alpha} = 1.0$ (i.e. no reverberation meaning that the room is not present – free field conditions).
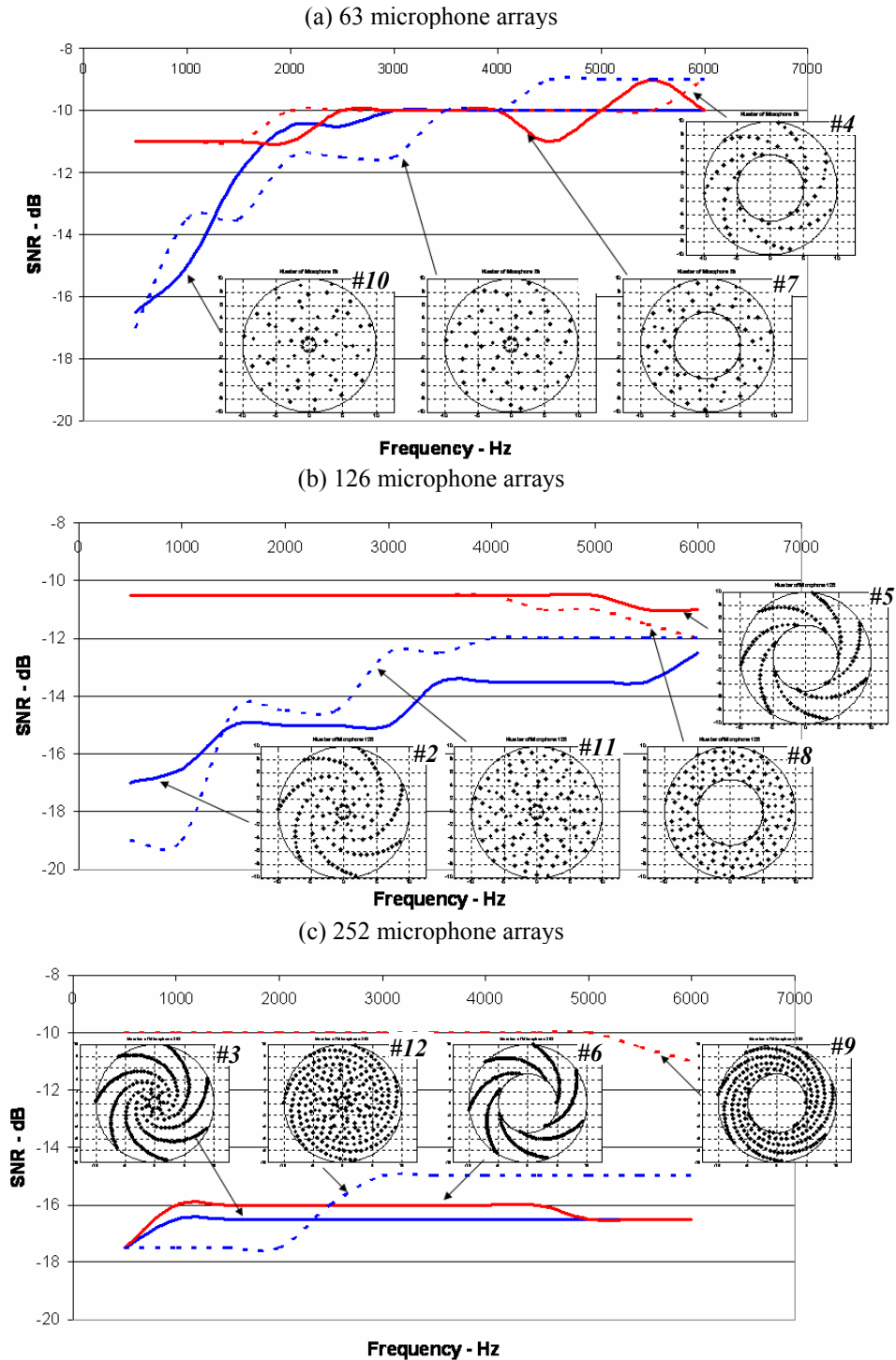
Figure 5: Signal to noise ratio (SNR) for the 12 microphone phased arrays investigated.

The SNR of the 12 microphone array designs investigated were computed and plotted as a function of frequency in Figure 5. The pattern of the arrays is shown in the figure and the design is indicated on the top-right corner of the array. From Figure 5a, it can be observed that the 63 microphone array designs provide ~ 10 dB of SNR. Array designs #10 and #1 provided better results at frequencies below 1500 Hz. By increasing the number of microphones to 126, the SNR is significantly improved reaching ~15 dB over a wider frequency range (< 3000 Hz) as shown in Figure 5b. For the arrays with 252 microphones, a SNR of ~ 16 dB can be achieved over the complete frequency range (array designs #3 and #6). Also, note the poor SNR for array design #9 even though it has 252 microphones. Finally, it can be observed that the array designs with an interior diameter of 10 meters are characterized by producing a nearly constant SNR vs frequency. From this study, the array design #2 with 126 microphones seems a reasonable compromise between having a large SNR (14-16 dB) and the number of microphones that determines the complexity and cost of the system.

The phased array beamwidth more commonly referred as "spot size" defines the capability of the array to separate sources spatially. The beamwidth is completely controlled by the outside dimension of the array. This fact is illustrated in the results shown in Figure 6 that presents the beamwidth as a function of the frequency for array designs 1 (63 microphones) and 2 (126 microphones). It can be observed that at low frequencies the beamwidth increases rapidly, e.g. at 100 Hz the beamwidth is 5 meters. To decrease the beamwidth, the array's outside diameter needs to be increased. For the machine health monitoring application, the machines to be monitored will need to be apart at least a beamwidth for the array to be able to distinguish the machines at a given frequency.
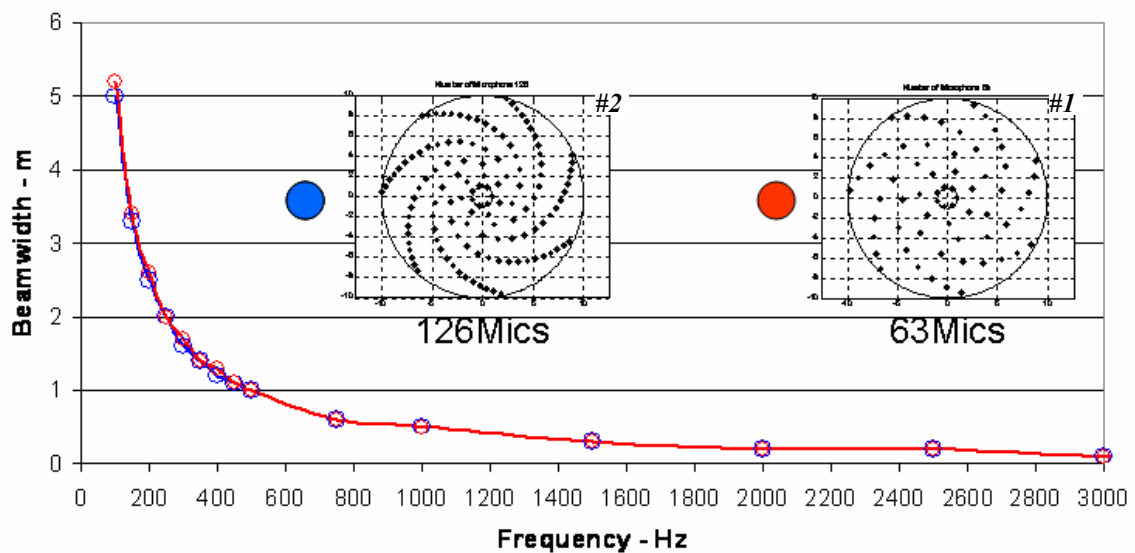
Figure 6: Beamwidth or spot size for array design #1 and #2 as a function of frequency.

3.2 Evaluation of Microphone Phased Array System

To demonstrate the potential of the proposed microphone phased array system, a simulation was carried out where 27 machines were monitored by a single array. The

machines were uniformly distributed in the room. Array design #2 was selected for these simulations. Figure 7 shows the room, the 27 machines to be monitored, and the array. The first reflection at the room walls and reverberation are included (absorption coefficient of $\bar{\alpha} = 0.1$). Each machine is modeled as a single noise source and all machines are assumed to generate the same noise levels (same acoustic power). Moreover, the machines' noise spectra are white noise (same level at all frequencies or flat noise spectrum). The acoustic images were computed for a frequency range from 100 to 6000 Hz. Figure 8 shows the acoustic images at 200, 500, and 1000 Hz computed over the whole room on the plane of the sources (3 meter above the floor).

(a) 3D View

(b) Top view
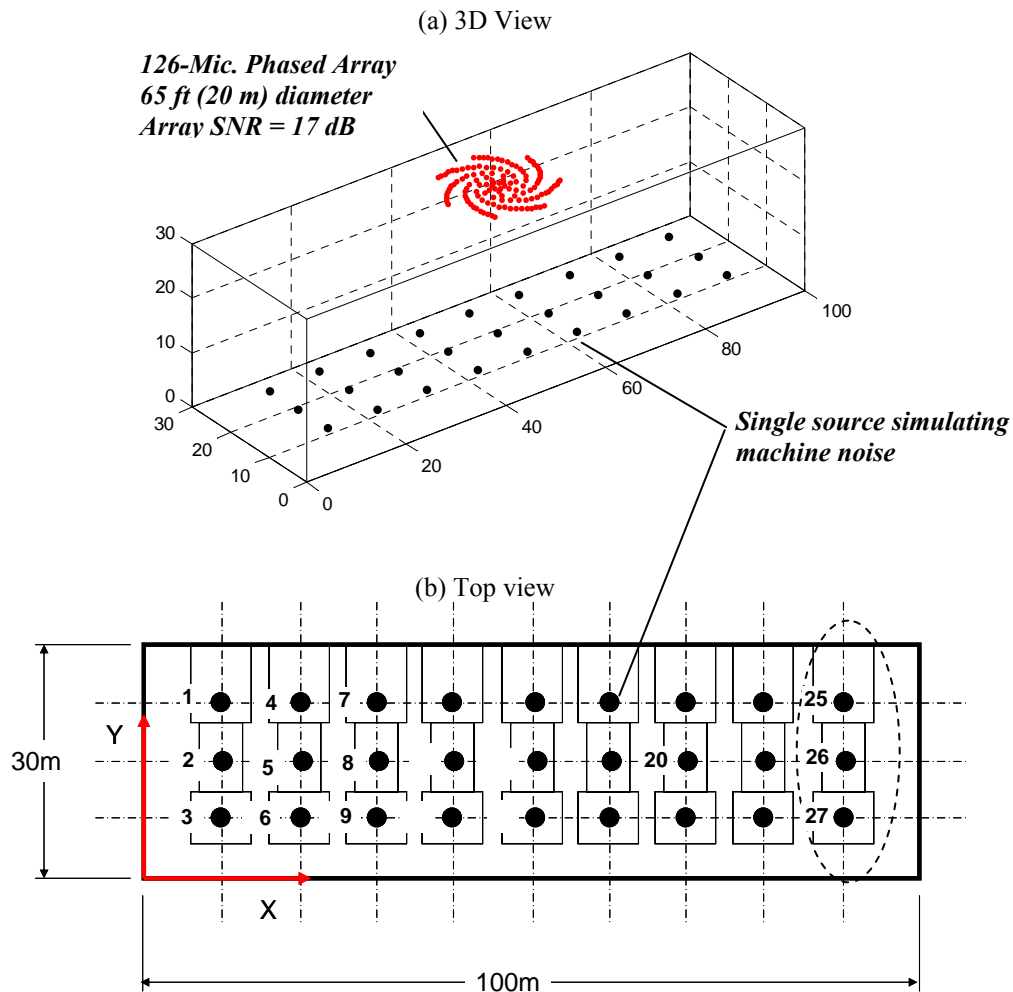
Figure 7: Machines (27) monitored by array design #2.

In Figure 8a, the results show that the array clearly is able to identify the 15 machines that are at the center of the room. The array fails to identify the machines towards the sides. Note that the last two units on both sides appear as single elongated sources (in the x-direction). However, at higher frequencies the array is capable to distinguish and thus monitor all 27 machines (noise sources) as shown in Figures 8b and c.

(a) 200 Hz

15 noise sources (machines) easily identified by the array

Array is not capable of identifying the sources towards the end of the room

Appears as a single noise source

(b) 500 Hz

Source #8
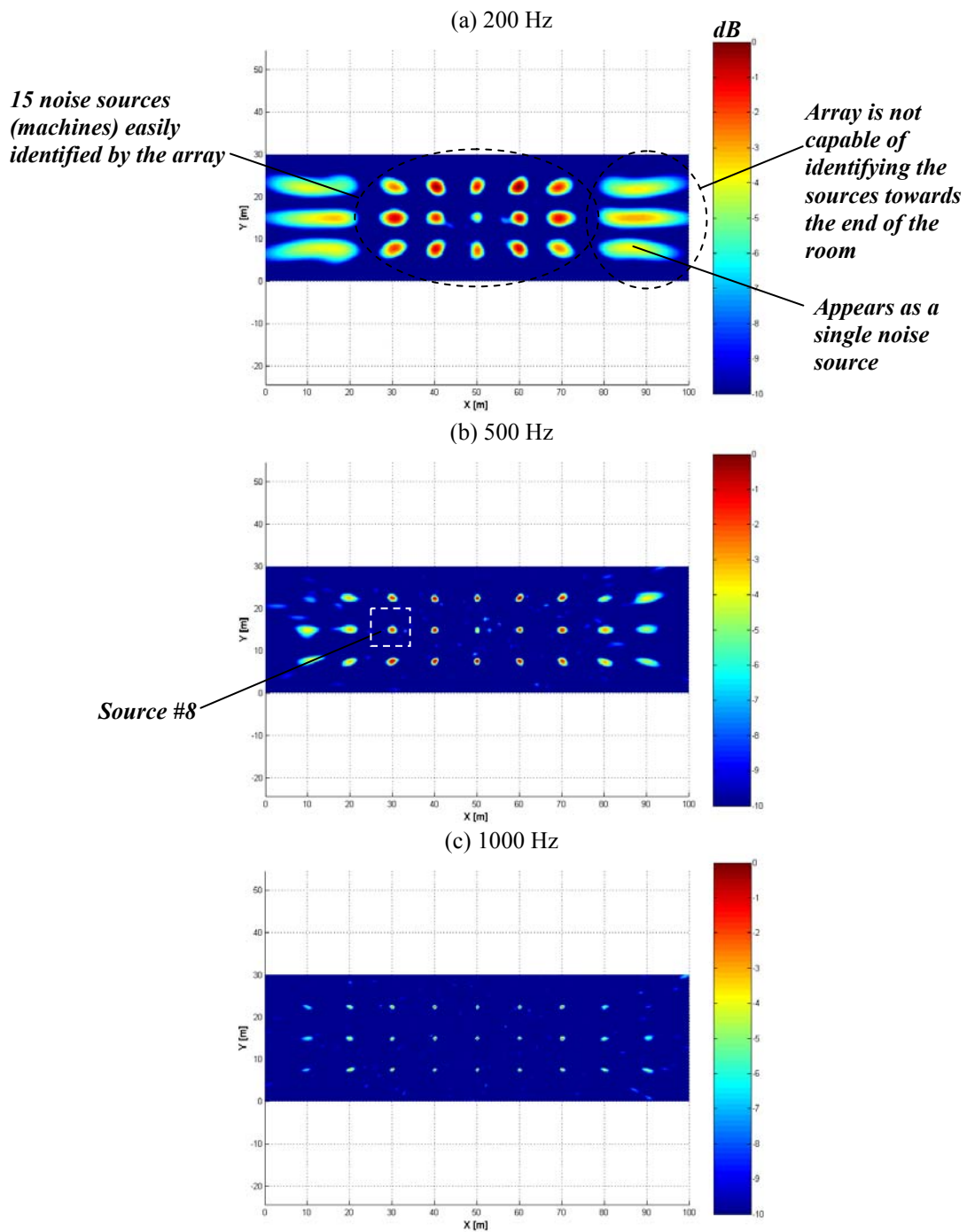
(c) 1000 Hz

Figure 8: Acoustic image for the whole room at (a) 200, (b) 500, and (c) 1000 Hz. Reflections included and absorption coefficient of $\bar{\alpha} = 0.1$. For ease of visualization, the acoustic map is normalized relative to maximum level.

3.3 Damage Simulation Examples

To further investigate the performance of the system, several damage scenarios were simulated. Figure 9 shows the integrated spectrum for the case of a single machine failure, e.g. an increase of the machine noise signature was used to determine if damage was identified. The damage scenario consisted of increasing the noise level for machine #23 by 2 dB (or equivalent to a gain in the signal by a factor of 1.25) while keeping all the other machines unchanged. Figure 9 shows the results indicating that machine #23 has been damaged. The integrated spectrum for this machine is shown in the bottom right corner. The blue curve corresponds to the spectrum before the 2 dB increase was simulated (e.g. healthy condition). This plot shows two interesting features. Firstly, the integrated spectrum increases rapidly below 100 Hz which is due to the lack of spatial resolution of the array at low frequencies. Secondly, the spectrum is modulated in the 50-250 Hz range which is the result of constructive/destructive interference produced by the wall reflections. The rest of the spectrum is essentially flat as expected. The second spectrum (red line) is the result of assuming a constant increase in the spectrum level of 2 dB to simulate damage.
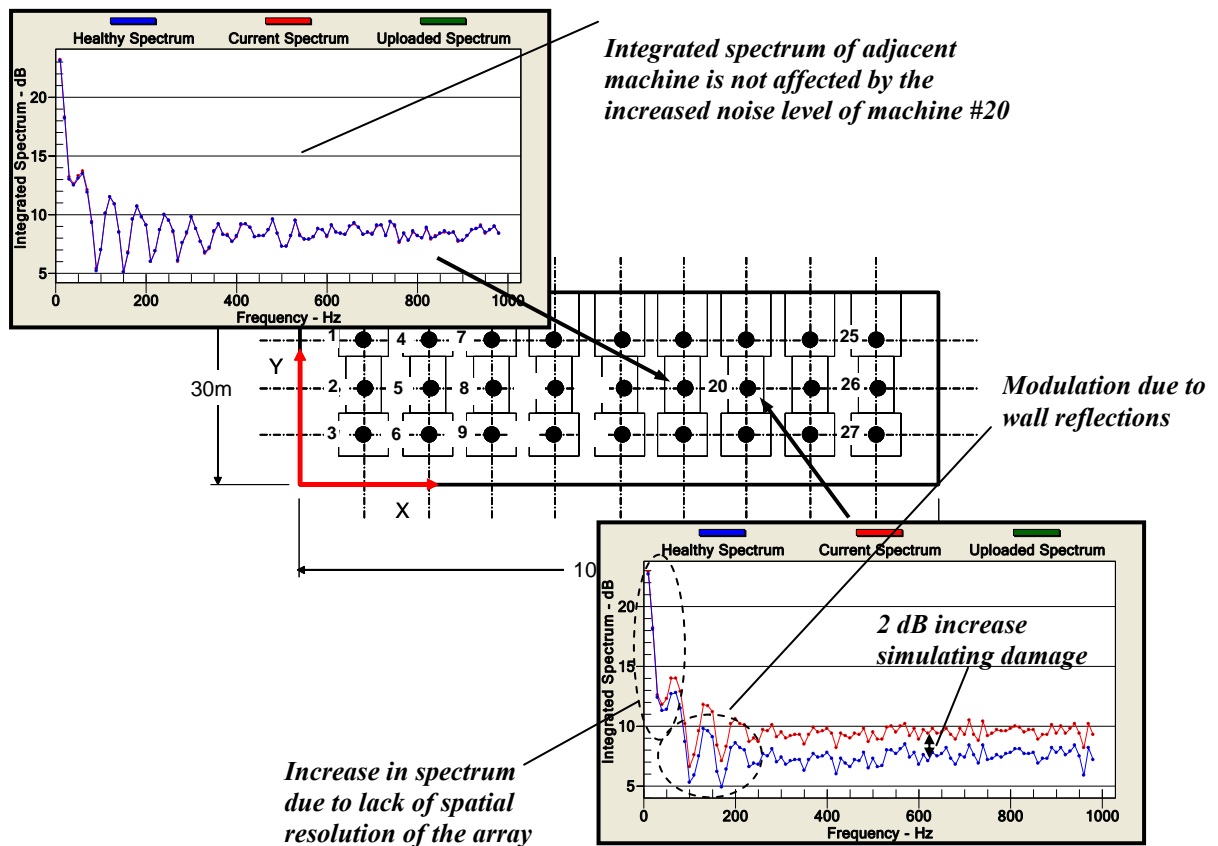
Figure 9: Results for single machine damage scenario. Damage simulated: the noise level of machine #20 was increased by 2 dB while all the others remain unchanged.

On the top left corner, the integrated spectrum of machine #20 is shown for both before (blue curve) and after (red curve) the 2 dB increase of machine #20 is simulated. It

can be seen that these two curves are virtually identical. This result shows that, even when the machines are adjacent, the microphone phased array system is clearly capable of separating the radiation from the individual machines. Plots of the integrated spectrum of all the other machines show the same conclusions.

These results presented here clearly indicate the capability of the microphone phased array system to correctly detect changes (or damage). Examples with multiple failures have also been investigated and shown good results (Ravetta et.al., 2006).

4   CONCLUSIONS

The main goal of this work was to develop a numerical tool to investigate the potential of acoustic imaging technology for the health monitoring of machinery in industrial environments. Several array designs were investigated and key limitations of the approach identified. The array SNR must be larger than the noise difference between the loudest and quietest machines being monitored: The array can "see" only sources that generate noise levels that are above the side-lobes of the loudest source in the room. A large diameter phased array is required to be able to identify noise sources at low frequencies. The study performed here shows that a 20 meter diameter array has a beamwidth of 2 meters at 200 Hz. The implication is that the noise sources must be physically separated at least 2 meters to be able to distinguish them at 200 Hz. At lower frequencies (< 200 Hz), the array must be even larger to separate sources. The reverberation of a typical equipment plant is not a critical issue. An array with sufficient number of microphones can effectively deal with the highly reverberant environment of typical equipment plants. It was demonstrated that an array with 126 microphones can effectively work in a highly reverberant acoustic room, i.e. with an absorption coefficient of just 0.1 or 10%. Similarly, the coherent reflections from the room walls are not a critical issue. Finally, a single microphone array positioned on the plant ceiling can monitor multiple machines.

REFERENCES

Bies, D.A. and Hansen, C.H., *Engineering Noise Control: Theory and Practice*, 3rd edition, Spon Press, 1986.

Brooks, T.F., Marcolini, M.A., and Pope, D.S., A Directional Array Approach for the Measurement of Rotor Noise Source Distributions with Controlled Spatial Resolution, *Journal of Sound and Vibration*, Volume 112, Number 1, pp. 192-197, 1987.

Grosche, F.R., Schneider, G., and Stiewitt, H., Wind Tunnel Experiments on Airframe Noise Sources of Transport Aircraft," *3rd AIAA/CEAS Aeroacoustics Conference*, Atlanta, GA, AIAA-97-1642-CP, 1997.

Herkes, W.H. and Stoker, R.W., Wind Tunnel Measurements of the Airframe Noise of a High-speed Civil Transport," *36th Aerospace Sciences Meeting and Exhibit*, Reno, NV, January 1998. AIAA 98-0472, 1998.

Johnson, D.H. and Dudgeon, D.E., *Array Signal Processing - Concepts and Techniques*, Prentice-Hall, NJ, 1993.

Mosher, M., Phased Arrays for Aeroacoustic Testing: Theoretical Development, *2nd AIAA/CEAS Aeroacoustics Conference*, State College, PA, AIAA 1996-1713. 1996.

Mueller T. (ed.), *Aeroacoustic Measurements*, Springer, ISBN 3-540-41757-5, 2002.

Ravetta, P.A., Burdisso, R.A., Ng, W.F., Wind Tunnel Aeroacoustic Measurements of a 26%-scale 777 Main Landing Gear Model, *10th AIAA/CEAS Aeroacoustics Conference and Exhibit,* , Manchester, United Kingdom. AIAA 2004-2885, May 2004.

Ravetta, P.A., Burdisso, R.A., and Anderson, J., *Microphone Phased Array Machinery Fault Diagnostic System*, AVEC Internal Report, March 2006.

Sijtsma, P. and Holthusen, H., Source Location by Phased Array Measurements in Closed Wind Tunnel Test Sections, *5th AIAA/CEAS Aeroacoustics Conference*, Bellevue, WA, AIAA 99-1814, 1999.